Broadband polarization correction with programmable liquid-crystal modulator arrays

M. Akbulut, R. Nelson, and A. M. Weiner

School of Electrical and Computer Engineering, Purdue University, West Lafayette, Indiana 47907-1285

P. Cronin and P. J. Miller

CRI, Inc., 35-B Cabot Road, Woburn, Massachusetts 01801

Received October 12, 2003

We demonstrate a novel method of parallel, multiwavelength state-of-polarization (SOP) correction. Using a new liquid-crystal modulator array design, we are able to rotate the distorted input SOP spectrum to a fixed linear state on a wavelength-by-wavelength basis. We report experimental correction of up to 25.5-dB polarization-dependent loss over a 13-nm bandwidth around 1550 nm. © 2004 Optical Society of America

OCIS codes: 060.2330, 260.5430, 320.5540, 230.3720, 230.6120, 230.5440.

The optical telecommunications community has lately been considering polarization effects such as polarization-mode dispersion (PMD) and polarization-dependent loss (PDL) as important bottlenecks in current and upcoming systems.[1] PMD arises from the random birefringences in single-mode fibers. This results in random, wavelength-dependent polarization transformations and delays that can lead to system outages.[2,3] The interaction of polarization-scrambled pulses and PDL further degrades system performance.[4] Current PMD compensators usually implement the idea of delaying orthogonal polarization states to reverse differential group delay (DGD), but this works only for a small bandwidth, which is inversely proportional to the mean DGD.[1,5,6] For broadband PMD and PDL compensation, fixing the wavelength-dependent state of polarization (SOP) is required as a first step. Motivated by this idea, we have devised a novel, broadband SOP corrector. By using a specially designed liquid-crystal modulator (LCM) array in an optical pulse-shaper setup,[7] we are able to transform wavelength-dependent arbitrary input SOP into a fixed linear state for all wavelengths. In experiments, we achieved correction of up to 25.5-dB spectral PDL over an approximately 13-nm bandwidth around 1550 nm.

When fixed-polarization broadband light is launched into a single-mode fiber, the SOP at the output of the fiber varies randomly with wavelength, depending on the PMD characteristics of the fiber.[2] To illustrate this, we constructed a simulation tool that approximates the single-mode fiber as a concatenation of 5000 equivalent wave plates that are randomly oriented. The input to this fiber had a Gaussian spectrum with ~6.66-nm intensity FWHM bandwidth. Figure 1 shows the output SOP spectra and power transmission spectra through a linear x polarizer for average DGDs of 3 and 20 ps, respectively. It is observed that, even for the smaller 3-ps mean DGD, SOP evolution versus wavelength is quite large, and there is a significant frequency-dependent PDL. It is important to correct such effects for high-capacity broadband transmission systems.

In our experiment (Fig. 2), a broadband amplified spontaneous emission source centered near 1550 nm was arbitrarily polarized with a Polarcor polarizer and a polarization controller. Then the polarized broadband light passed through a SOP-distorting element. The various types of SOP distorters that we tested were one piece of polarization-maintaining (PM) fiber, two equal-length pieces of PM fiber concatenated with a 23° angle offset, two mismatched-length pieces of PM fiber concatenated with a 35° angle offset, and five pieces of PM fiber with random lengths and concatenation angles. The total lengths of one- and two-piece PM fibers were ~2.6 m. We

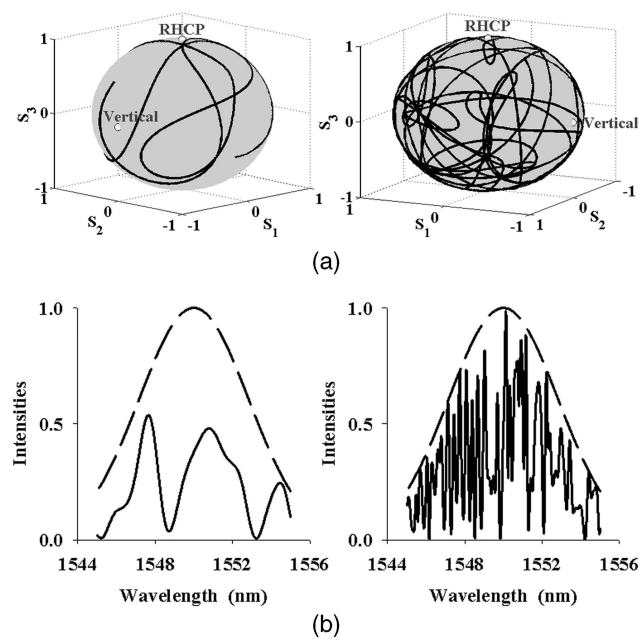

Fig. 1. Simulation of SOP versus wavelength evolution (top row) and PDL (bottom row; the dashed curves represent the input power spectra, and the solid curves represent the output power spectra after a linear x polarizer) as a result of PMD. The left-hand column is for 3-ps mean DGD, and the right-hand column is for 20-ps mean DGD. RHCP, right-hand circular polarization.

0146-9592/04/101129-03$15.00/0

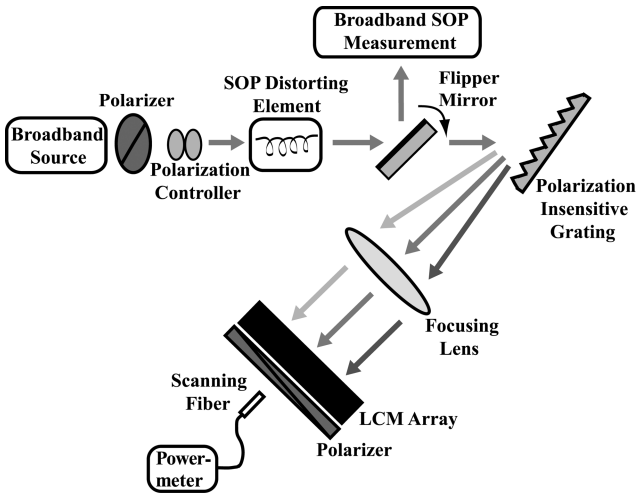

Fig. 2. Experimental setup.

intentionally kept these lengths constant to observe the effects of individual piece length and angle between the pieces. The five-piece PM case was ~1.69 m long. The one-piece PM fiber functions as a simple wave plate that produces a cyclic evolution of SOP versus wavelength, whereas the two- and five-piece PM cases are expected to produce more-complicated SOP spectra.

To be able to correct SOP, first we have to know what it is. For this purpose we constructed a broadband polarization measurement apparatus by modifying a commercial single-frequency polarimeter. After the SOP-distorting element, the beam enters the first half of a single-pass pulse-shaper setup,[7] where it is diffracted by a polarization-insensitive grating and focused uniformly on the LCM pixels. The grating and lens were chosen to image an ~14-nm bandwidth across the 12.8-mm aperture of the LCM array. We mimic PDL by inserting a polarizer after the LCM. In the future we intend to remove the polarizer and put a mirror after the LCM to convert our setup into a double-pass pulse shaper.[8] Finally, the power transmission spectrum is measured by scanning a single-mode fiber (connected to a powermeter) with a motorized translation stage over the aperture of the LCM array. Computer control of the translation stage, the LCM, and the powermeter provides a robust experimental environment.

The LCM array consists of two individually controllable layers with 128 independent pixels at each layer. Each pixel is 100 μm wide. Each layer was individually calibrated for voltage versus retardation. The device that we are using is similar to those used in phase-and-amplitude pulse shaping[9] but with the liquid-crystal geometry modified to permit transformation of arbitrary input SOP into a linear output SOP. The traditional two-layer LCM arrays use a $+45°/-45°$ orientation for the voltage-controllable crystal axis. This does not allow mapping of arbitrary input SOP to a single fixed output polarization state. Our special LCM array utilizes a $+90°/-45°$ orientation to cover the whole Poincaré sphere. Any SOP point on the sphere can be transformed into either vertical or horizontal polarization by applying appropriate retardations to the LCM layers. The first layer rotates the input SOP on the Poincaré sphere around the S_1 axis to a point on the great circle that goes through the poles and the vertical–horizontal polarizations. Then the second layer rotates around the S_2 axis to its destination point. In our experiments we chose this point to be the vertical polarization. To be able to rotate input SOP arbitrarily to any state, one would need a third liquid-crystal layer[10]; however, this functionality is not required for correction of wavelength-dependent SOP.

Figures 3 and 4 show the SOP versus wavelength measurement on the Poincaré sphere and the power spectrum after the output polarizer. The deeply modulated curves in the right-hand columns are

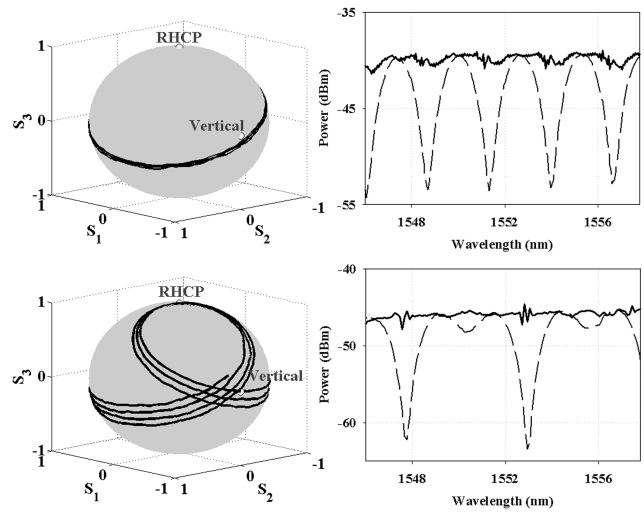

Fig. 3. SOP spectra before the pulse-shaper setup (left) and power spectra after the LCM + polarizer for uncorrected (dashed curve) and corrected (solid curve) SOP versus wavelength (right). The SOP distorters are a one-piece PM fiber (top row) and an equal-length two-piece PM fiber (bottom row).

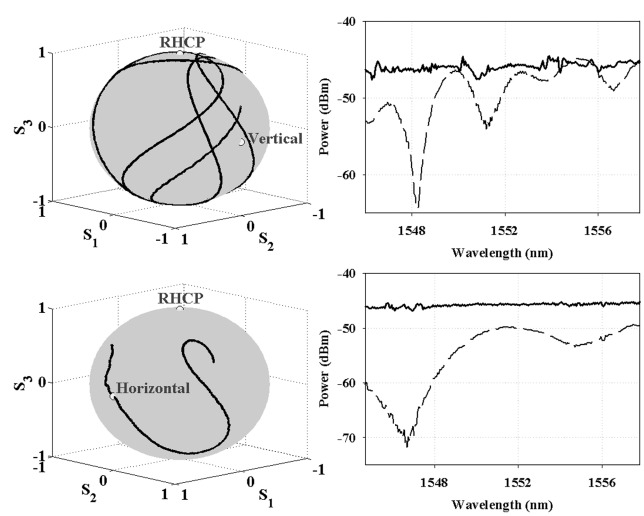

Fig. 4. Same as Fig. 3, but the SOP distorters are a mismatched-length two-piece PM fiber (top row) and a five-piece PM fiber (bottom row).

obtained by setting all the LCM pixels to a fixed retardation (the fixed value is 2π in the two- and five-piece PM cases, so the LCM does not change the polarization), and the flatter ones are obtained with the correction algorithm applied. For the basic SOP distorter, namely, the one-piece PM fiber, we show 12.5-dB PDL correction (Fig. 3). Also, the equal-length two-piece PM case with 18-dB correction is shown in Fig. 3. Additionally, for this two-piece PM fiber, we observed that changing the input polarization did not disturb our ability to correct PDL. Figure 4 shows more-complex SOP versus wavelength structures. In particular, the five-piece PM fiber is a better imitation of PMD than the one- and two-piece PM fibers. The top row is for the mismatched-length two-piece PM fiber, and the bottom row is for the five-piece PM fiber; 19- and 25.5-dB corrections are observed, respectively.

The 1–2-dB residual PDL that are apparent on the corrected curves of Figs. 3 and 4 can be tied to a few reasons. Because of errors in the broadband SOP measurement, our algorithm would predict incorrect polarization transformations and thus a nonflat power spectrum. Another reason is the resolution of the pulse-shaper system. If the SOP is varying rapidly over some small frequency band, then the spectral resolution may not be fine enough to correct it for the entire frequency band. Finally, our measurement scheme involving a scanning fiber to sample the spatially dispersed optical frequencies may be influenced by diffraction effects that result from the finite distance between the LCM planes and the sampling fiber.

Note that in this Letter we focus on wavelength-dependent SOP compensation and do not address spectral phase or temporal behavior. For the case of an optical pulse input, PMD causes not only wavelength-dependent SOP but also input-polarization-dependent and wavelength-dependent delay. Wavelength-dependent delays are equivalent to spectral phase variations. Also, in the process of our SOP correction, the two-layer LCM that we use will impart additional spectral phase variations onto the signal that add to those introduced by PMD. Compensation of time-domain distortions will require correction of the overall spectral phase variations subsequent to the SOP correction demonstrated in this Letter. This can potentially be accomplished in future experiments, for example, by coupling the output of a full double-pass SOP compensator setup to a second pulse shaper functioning as a spectral phase equalizer. Such spectral phase equalization with pigtailed pulse shapers was demonstrated earlier.[8,11] We note that such phase-only pulse shapers have been successfully implemented with fiber-to-fiber insertion loss of 5.1 dB (Ref. 8); this enhances the possibility of full PMD compensation via concatenated spectral SOP correction and spectral phase correction in future experiments.

Another application that may benefit from our LCM array is the generation of arbitrary SOP spectra from an input spectrum with a fixed linear SOP. This is exactly our SOP correction algorithm run backward. The SOP spectrum synthesis can also be done in a time-dependent fashion by continuously programming the LCM array. The speed of course will be dependent on liquid-crystal response times and the other components in the setup. Polarization pulse shaping by use of conventional $+45°/-45°$ LCM arrays was reported before.[12] However, the geometry of these conventional arrays limits the possible wavelength-dependent SOPs to an arc on the Poincaré sphere. In contrast, our device has the potential of producing wavelength-dependent SOPs that cover the entire sphere (although an additional degree of freedom would be needed for spectral phase control, which is very important for ultrafast optical pulse-shaping applications). Furthermore, our LCM array could be used (without the grating) to produce monochromatic fields with arbitrary, one-dimensional spatially varying polarization states.

In summary, we have demonstrated a new scheme for broadband SOP correction. The advantages of this scheme are the ability to correct arbitrary input polarizations and to do so on a wavelength-by-wavelength basis even for moderately large bandwidths. Further work will involve extending the setup to a double-pass geometry (similar to pulse shaping[7,8]), with all wavelengths going back into a single fiber, and investigating spectral delay correction to achieve a full, broadband PMD compensator.

This work was funded by the National Science Foundation under grant 0140682-ECS. M. Akbulut's e-mail address is ma@purdue.edu.

References

1. A. E. Willner, in *Digest of the IEEE LEOS Summer Topical Meetings* (Institute of Electrical and Electronics Engineers, Piscataway, N.J., 2003), Polarization Mode Dispersion section, p. 3.
2. C. D. Poole and J. Nagel, in *Optical Fiber Telecommunications IIIA*, I. P. Kaminow and T. L. Koch, eds., (Academic, San Diego, Calif., 1997), p. 114.
3. H. Bülow, IEEE Photon. Technol. Lett. **10,** 696 (1998).
4. N. Gisin and B. Huttner, Opt. Commun. **142,** 119 (1997).
5. M. Shtaif, A. Mecozzi, and J. A. Nagel, IEEE Photon. Technol. Lett. **12,** 53 (2000).
6. H. Bülow, in *Digest of Optical Fiber Communication Conference* (Optical Society of America, Washington, D.C., 1999), p. 74.
7. A. M. Weiner, Rev. Sci. Instrum. **71,** 1929 (2000).
8. R. D. Nelson, D. E. Leaird, and A. M. Weiner, Opt. Express **11,** 1763 (2003), http://www.opticsexpress.org.
9. M. M. Wefers and K. A. Nelson, Opt. Lett. **20,** 1047 (1995).
10. Z. Zhuang, S. Suh, and J. S. Patel, Opt. Lett. **24,** 694 (1999).
11. C. C. Chang, H. P. Sardesai, and A. M. Weiner, Opt. Lett. **23,** 283 (1998).
12. T. Brixner and G. Gerber, Opt. Lett. **26,** 557 (2001).